Photo-induced oxidation of [Fe-II(N4P(y))CH3CN] and related complexes

Draksharapu, Apparao; Li, Qian; Roelfes, Gerard; Browne, Wesley R.

Published in:
Dalton Transactions

DOI:
10.1039/c2dt30392b

Publication date:
2012

Dalton Transactions

Cite this: *Dalton Trans.*, 2012, **41**, 13180

www.rsc.org/dalton

PAPER

Photo-induced oxidation of $[Fe^{II}(N4Py)CH_3CN]$ and related complexes†‡

Apparao Draksharapu, Qian Li, Gerard Roelfes and Wesley R. Browne*

Received 19th February 2012, Accepted 22nd March 2012
DOI: 10.1039/c2dt30392b

The photochemistry of the complexes $[Fe(N4Py)(CH_3CN)](ClO_4)_2$ (**1**), where N4Py is 1,1-di(pyridin-2-yl)-*N*,*N*-bis(pyridin-2-ylmethyl)methanamine and $[Fe(MeN4Py)(CH_3CN)](ClO_4)_2$ (**2**), where MeN4Py is 1,1-di(pyridin-2-yl)-*N*,*N*-bis(pyridin-2-ylmethyl)ethanamine, in water, dichloromethane and methanol is described. Under UV or visible irradiation both **1** and **2** undergo enhancement of the rate of outer sphere electron transfer to $^3O_2$ to yield the superoxide radical anion and the complexes in the Fe(III) redox state. Addition of ascorbic acid to the photoproduct leads to a recovery of the initial UV/Vis spectrum of **1** and **2**, indicating that ligand oxidation does not occur. The results are discussed within the context of the recent report of the enhancement of the oxidative DNA cleavage activity of **1** under UV and visible irradiation (*Inorg. Chem*. 2010, **49**, 11009).

Introduction

Whereas, even after more than half a century, the photochemistry of Ru(II) polypyridyl complexes continues to receive attention,[1] studies of the photochemistry of electronically analogous Fe(II) polypyridyl complexes are relatively scarce.[2–4] This disparity is in large part due to the differences in the excited state electronic structure of Ru(II) and Fe(II) complexes.[5] For the invariably low spin Ru(II) polypyridyl complexes the lowest electronically excited states tend to be relatively long lived (50 ns to 10 μs) ^{3}MLCT (metal to ligand charge transfer) states.[1] The photochemistry of these complexes is dominated by radiative and non-radiative relaxation, thermal population of ^{3}MC (metal centred) states leading to ligand dissociation and photoinduced electron transfer (both oxidative and reductive). By contrast the photochemistry of Fe(II) polypyridyl complexes (which can be in either $^1A_1$ or $^5T_2$ ground states) is substantially hindered due to the lowest excited electronic states being MC rather than MLCT.[5] As a consequence the excited states are deactivated rapidly (<100 ps) to the ground state potential energy surface either directly to the $^1A_1$ state in the case of low spin Fe(II) complexes or *via* a series of higher energy microstates, as demonstrated most elegantly in the LIESST effect by Hauser and co-workers and others.[6] The rate of these processes renders other excited state relaxation channels such as emission, photo-dissociation and photoinduced electron transfer uncompetitive and hence, apart from photo-dissociation,[7] they are not usually observable. Despite this, several groups have shown that certain low spin Fe(II) polypyridyl complexes have sufficient long lived low energy excited states (10 to 100 ns at room temperature) to show photochemistry such as reversible ligand dissociation.[4]

In the present contribution we describe the photochemistry of the complex $[Fe(N4Py)(CH_3CN)]^{2+}$ (**1**)[8] and its methylated analogue $[Fe(MeN4Py)(CH_3CN)]^{2+}$ (**2**)[9] (Fig. 1) in aqueous and non-aqueous solvents. We show that upon excitation with visible or UV light, outer sphere electron transfer to $^3O_2$ occurs to form the corresponding Fe(III) complex (*e.g.*, **3**) and the superoxide radical anion.

Complex **1** is one of the most active iron based oxidation catalysts reported in the cleavage of DNA with $^3O_2$ as terminal oxidant.[8b] Recently we demonstrated that the activity of **1** in the cleavage of DNA was enhanced dramatically by irradiation with both UV and visible light.[10] Mechanistic probes suggested that although the activity was increased, in the case of irradiation with visible light, the mechanism of oxidation, *i.e.* the formation of superoxide from $^3O_2$, remained the same as observed for **1** in the absence of light. Furthermore we demonstrated[9] recently by

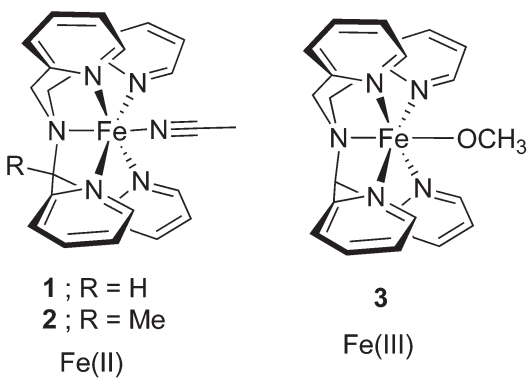

1 ; R = H
2 ; R = Me
Fe(II)

3
Fe(III)

Fig. 1 Structures of complexes **1**, **2** and **3**.

Stratingh Institute for Chemistry, Faculty of Mathematics and Natural Sciences, University of Groningen, Nijenborgh 4, 9747 AG Groningen, The Netherlands. E-mail: W.R.Browne@rug.nl

†Based on the presentation at Dalton Discussion No. 13, 10–12 September 2012, University of Sheffield, UK.

‡Electronic supplementary information (ESI) available: Additional ^{1}H NMR and UV/Vis absorption spectroscopic data. See DOI: 10.1039/c2dt30392b

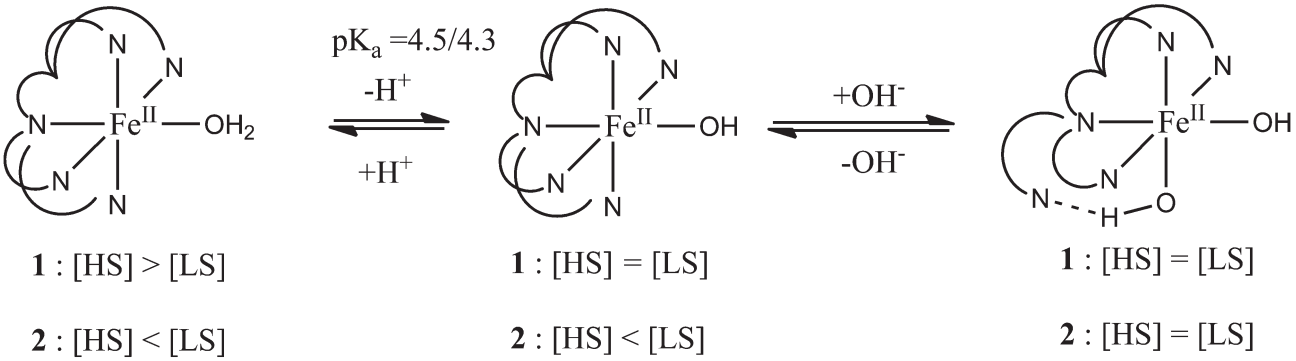

Scheme 1 Relative ratios of singlet and high spin state species for each species for **1** and **2**.[9]

a combination of UV/Vis, Raman and ^{1}H NMR spectroscopy and electrochemistry that the chemistry of **1** in aqueous media was dominated by two sets of equilibria in the pH range of relevance to the DNA cleavage studies (Scheme 1). The occurrence of both an equilibrium between two distinct complexes and in each case two distinct microstates suggested that the remarkable activity of **1** could be due to these spin equilibria, which transiently remove the barrier to electron transfer to $^3O_2$ *via* an intermediate triplet state and that the enhancement observed by irradiation could be due to an increase in the steady state population of such higher lying triplet states.

The aim of the present contribution is to understand the origin of the photo-enhancement of DNA cleavage activity, which necessitates the study of the photochemistry of complex **1** itself in aqueous and non-aqueous media.

Experimental

The ligands N4Py and MeN4Py and the complexes [Fe(N4Py)-$(CH_3CN)](ClO_4)_2$ (**1**), [Fe(MeN4Py)$(CH_3CN)](ClO_4)_2$ (**2**) and [Fe(N4Py)$(OCH_3)](ClO_4)_2$ (**3**) were available from earlier studies.[9,11] Commercially available chemicals were used without further purification unless stated otherwise. Solvents for electrochemical and spectroscopic measurements were UVASOL grade (Merck) or better.

Physical methods

UV/Vis absorption spectra were recorded with a Specord600 (AnalytikJena) spectrophotometer in 1 cm path length quartz cuvettes. ^{1}H NMR spectra (400.0 MHz) were recorded on a Varian Mercury Plus. Chemical shifts are denoted relative to the solvent residual peak (^{1}H NMR spectra CD_2Cl_2: 5.32 ppm). Electrochemical measurements were carried out using a model CHI760B Electrochemical Workstation (CH Instruments). Analyte concentrations were typically 0.5–1.0 mM in water containing 0.1 M KNO_3 or in organic solvents with 0.1 M $TBAPF_6$. Unless stated otherwise, a 3 mm diameter Teflon-shrouded glassy carbon working electrode (CH Instruments), a Pt wire auxiliary electrode, and an Ag/AgCl reference electrode were employed. Cyclic voltammograms were obtained at sweep rate of 100 mV s^{-1}. All potentials (±10 mV) are quoted with respect to the Ag/AgCl. Spectroelectrochemistry was carried out using a homemade electrolysis cell (a 2 mm pathlength quartz cuvette with a 3 cm by 1 cm platinum gauze, a Ag/AgCl reference electrode and platinum counter electrode) or an OTTLE cell[12] (a liquid IR cell modified with Infrasil windows, a platinum mesh working and counter electrode and a Ag/AgCl reference electrode) mounted in a Specord600 UV/Vis spectrometer with potential controlled by a CHI760C potentiostat. EPR spectra (X-band, 9.46 GHz) were recorded on a Bruker ECS106 spectrometer in liquid nitrogen (77 K). Samples for measurement (0.25 mL) were transferred, after irradiation or electrolysis, to EPR tubes, which were frozen in liquid nitrogen immediately. Raman spectra were obtained in a 180° backscattering arrangement with excitation at 561 nm (100 mW at source, Cobolt Lasers) and 473 nm (100 mW at source, Cobolt Lasers) with Raman scattering collected and collimated and subsequently refocused *via* a pair of 2.5 cm diameter plano-convex lens (f = 10 cm). The collected light was filtered by an appropriate long pass edge filter (Semrock) and dispersed by a Shamrock300i spectrograph (Andor Technology) with a 1200 l mm^{-1} grating blazed at 500 nm, or 1800 l mm^{-1} blazed at 400 nm and acquired with an DV420A-BU2 CCD camera (Andor Technology). The slit width was set to 10 or 20 μm. Data were recorded and processed using Solis (Andor Technology) with spectral calibration performed using the Raman spectrum of acetonitrile–toluene 50 : 50 (v : v). Samples were held in quartz 10 mm path length cuvettes. Solvent subtraction and a multipoint baseline correction were performed for all spectra. The concentrations used for resonance Raman studies were 0.25–0.5 mM. Singlet oxygen emission spectra were recorded using a 512 element InGaAs diode array detector (iDus, Andor Technology) cooled to −60 °C coupled to a Shamrock163 spectrograph with a 150 l mm^{-1} grating blazed at 1250 nm. Light collection was through a fibre optic cable with the sample held in a fibre coupled cuvette holder (Thorlabs) and excitation with a 200 mW (at sample) 532 nm laser (Cobolt) at 90°. Irradiation of solutions of **1**, **2** and **3** was carried out using either a 312 nm or 365 nm

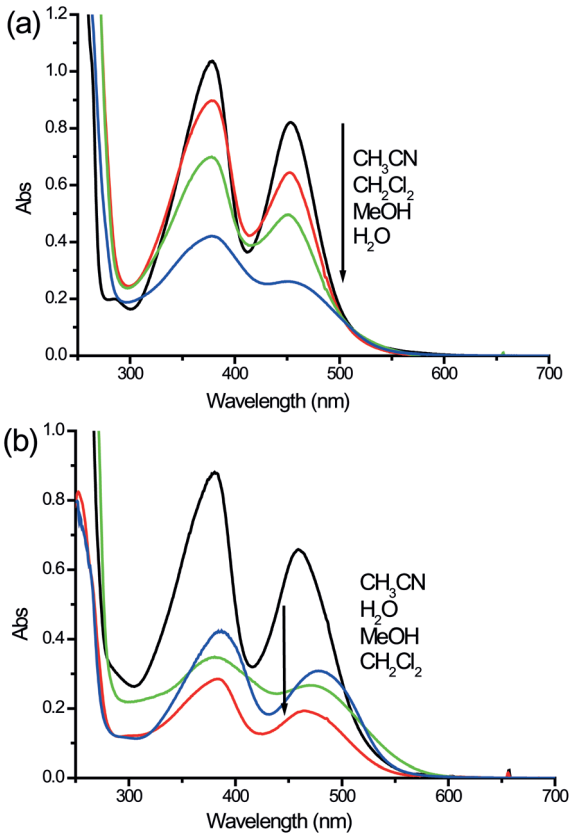

Fig. 2 UV/Vis absorption spectra of (a) **1** and (b) **2** in acetonitrile, dichloromethane, methanol and water (0.25 mM).

Spectroline black light, a 400 nm CW laser (Powertechnology, 35 mW at sample) or a medium pressure Hg lamp with a 400 nm long pass filter.

Results

The UV/Vis spectroscopy and electrochemistry of **1** and **2** in acetonitrile and in aqueous media were described earlier.[9] For both complexes the absorption spectrum in acetonitrile is typical of a low spin Fe(II) complex with two strong ^{1}MLCT transitions in the visible region and ligand $\pi-\pi^*$ transitions in the UV.[9] In aqueous solution the CH_3CN ligand dissociates fully with the result of a 20–50% (pH dependent) decrease in the molar absorptivity in the visible region. The shift and decrease in absorption is consistent with solvolysis in the case of water and methanol. The decrease in visible absorption of **1** in dichloromethane and methanol solution is less than that observed in water (Fig. 2a). Furthermore there is only a minor red-shift of the two visible absorption bands. By contrast for **2** a red-shift and a similar decrease in absorbance is observed in dichloromethane, methanol and water (Fig. 2b). In dichloromethane the displacement of the CH_3CN ligand with residual water occurs rather than solvolysis. This is confirmed by the ^{1}H NMR spectrum (see ESI Fig. S1‡) of **1** in CD_2Cl_2 in which two species are observed, one of which is the diamagnetic complex **1** with the CH_3CN ligand coordinated, and the other a paramagnetic species with a spectrum similar to that observed for the complex $[Fe(N4Py)(OH_2)]^{2+}$ in water at low pH.[9] In water saturated dichloromethane

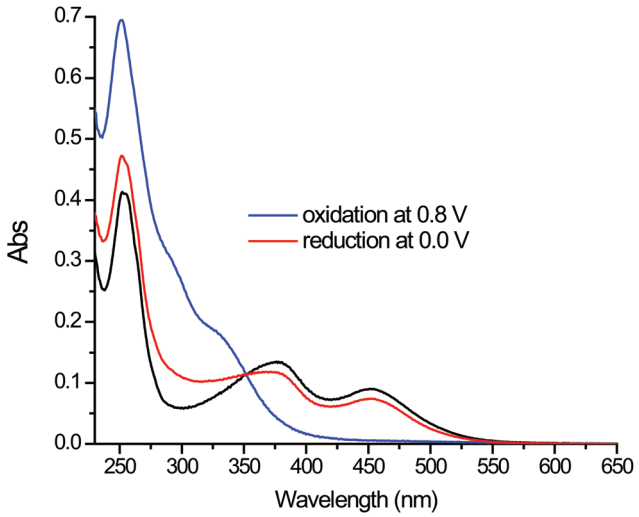

Fig. 3 Electrochemical oxidation of **1** at 0.8 V and subsequent reduction at 0.0 V *vs*. Ag/AgCl at pH 7 (0.1 M KNO_3). Initial spectrum in black.

the visible absorption bands decrease in intensity and undergo a red-shift (Fig. S2‡) and only a paramagnetic species is observed in the ^{1}H NMR spectrum (Fig. S1‡). The similarity of the UV/Vis absorption and ^{1}H NMR spectra in the presence of water indicate complete displacement of CH_3CN with $^-OH/H_2O$ (Fig. S1‡).

The cyclic voltammetry of **1** and **2** have been described previously in acetonitrile and water.[9] Briefly, the redox chemistry of both **1** and **2** is characterised by a reversible one electron oxidation at *ca.* 1.1 V in acetonitrile and, depending on the pH, at between −0.1 and 0.6 V in water. In addition, oxidation of **1** or **2** to the Fe(III) redox state in acetonitrile in the presence of water results in immediate exchange of the CH_3CN ligand for H_2O or OH^-.[9]

UV/Vis absorption spectroelectrochemistry

In earlier studies using complex **1** to cleave DNA with $^3O_2$ as terminal oxidant, oxidation to the Fe(III) state occurs with subsequent (chemical) reduction to the Fe(II) state required to complete the catalytic cycle.[10] Under irradiation with visible light (*e.g.*, at 400 nm) the activity of **1** was increased dramatically but with no apparent change in the overall mechanism.[10] Complexes **1** and **2**, and the species they form in aqueous solution, have been characterised in the Fe(II) oxidation state in our earlier studies.[9] The spectroscopic properties of the complexes in the Fe(III) state have not been reported in detail, however, and hence in order to establish if complexes formed upon irradiation of **1** and **2** are the same as formed upon (electro)chemical oxidation, *in situ* oxidation of **1** and **2** to the Fe(III) state was carried out in the present study by both chemical and electrochemical oxidation in acetonitrile and in water at various pH values. The Fe(III) species formed were characterised by UV/Vis absorption and EPR spectroscopy.

The UV/Vis absorption spectra of **1** and **2** in water before and after electrochemical oxidation and after reduction are shown in

Fig. 3 (see also ESI Fig. S3 and S4‡). Both **1** and **2** show two bands in the visible region in the Fe(II) oxidation state. Upon electrochemical oxidation at 0.6 V *vs*. Ag/AgCl the absorbance of these bands decreases and a new band grows in at 310 nm, with isosbestic points maintained. For **1** the original spectra were recovered upon reduction at 0.0 V at pH 2.5 and pH 7.6. At pH 10 the spectrum did not recover upon reduction, consistent with irreversible ligand dissociation (Fig. S3‡).[9] For **2**, by contrast, the original spectrum was recovered even at pH 10.5 (Fig. S4‡). Similar changes were observed upon oxidation and reduction with cerium(IV) sulphate and ascorbic acid, respectively (Fig. S5‡).

In acetonitrile, complexes **1** and **2** are oxidised at 1.2 V, however, full recovery of the original spectrum occurred only upon reduction at 0.4 V (Fig. 4), in agreement with previous studies in which it was demonstrated that upon oxidation the CH_3CN ligand is displaced by H_2O.[9] The red-shift in the near-UV absorption band of the Fe(III) complexes compared to water is indicative that in acetonitrile the sixth ligand is H_2O and not OH^- as in water at pH > 2. Addition of 2 vol% of water prior to oxidation resulted in the spectrum of the Fe(III) complex formed being similar to that obtained in water at pH 7.6.

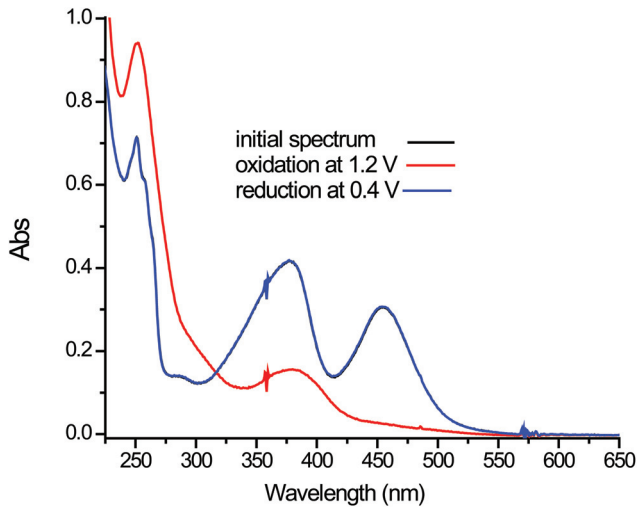

Fig. 4 Electrochemical oxidation of **1** at 1.2 V and subsequent reduction at 0.4 V *vs*. Ag/AgCl in acetonitrile solution (0.1 M $TBAPF_6$). Note that the initial spectrum in black and final spectrum in blue are almost identical.

Characterisation of **1** and **2** in the Fe(III) state by EPR spectroscopy was achieved by preparative bulk electrolysis followed by flash freezing of samples in liquid nitrogen. The bulk electrolysis was monitored *in situ* by UV/Vis spectroscopy. Samples prepared by bulk electrolysis in water at pH 2 were EPR silent at 77 K (Fig. S6‡). At pH 3.9 and 6.6 two sets of signals, which are characteristic for high and low spin Fe^{III} species, are observed (Fig. 5 and Fig. S7‡). At high pH only one signal corresponding to a high spin Fe^{III} complex is observed, which together with the irreversibility of the oxidation at this pH (*vide supra*), indicates formation of free Fe(III) (*i.e.* ligand loss, Fig. S8‡).

Aerobic oxidation of 1 and 2

In acetonitrile the UV/Vis absorption spectra of **1** and **2** remained unchanged for at least several days. By contrast in dichloromethane, methanol or aqueous solutions oxidation to the Fe(III) redox state was observed. The rate of oxidation in water was found to be pH dependent with oxidation proceeding faster under acidic conditions (pH <4) than at near-neutral pH (4–8) (Fig. S9‡). In general the rate of aerobic oxidation of **2** was at least an order of magnitude less than that of **1**.

Photochemistry of 1 and 2

The photochemistry of **1** and **2** was examined in methanol, water, dichloromethane, ethanol and acetonitrile. In acetonitrile,

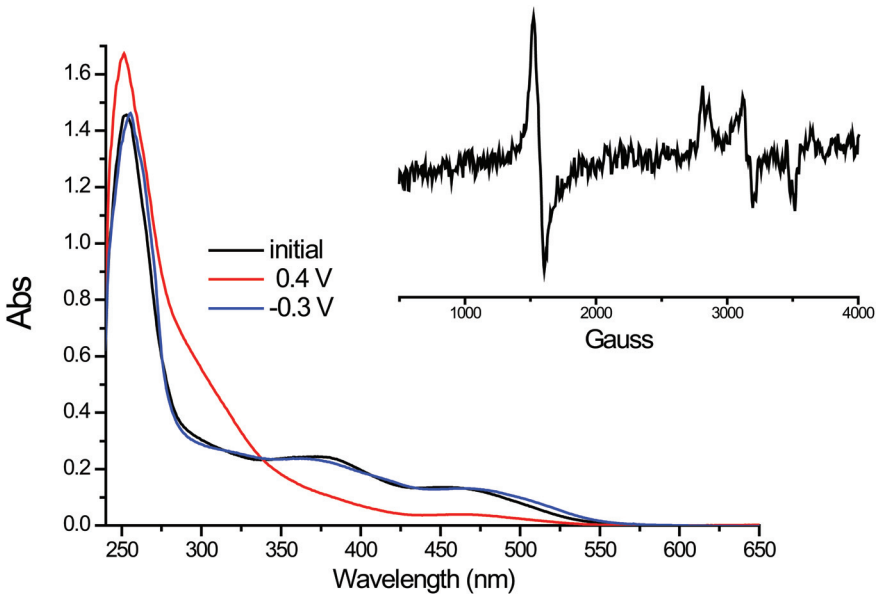

Fig. 5 UV/Vis absorption spectroelectrochemistry of **1** in water at pH 6.6 and (inset) *ex situ* EPR spectrum of the solution after oxidation at 0.4 V.

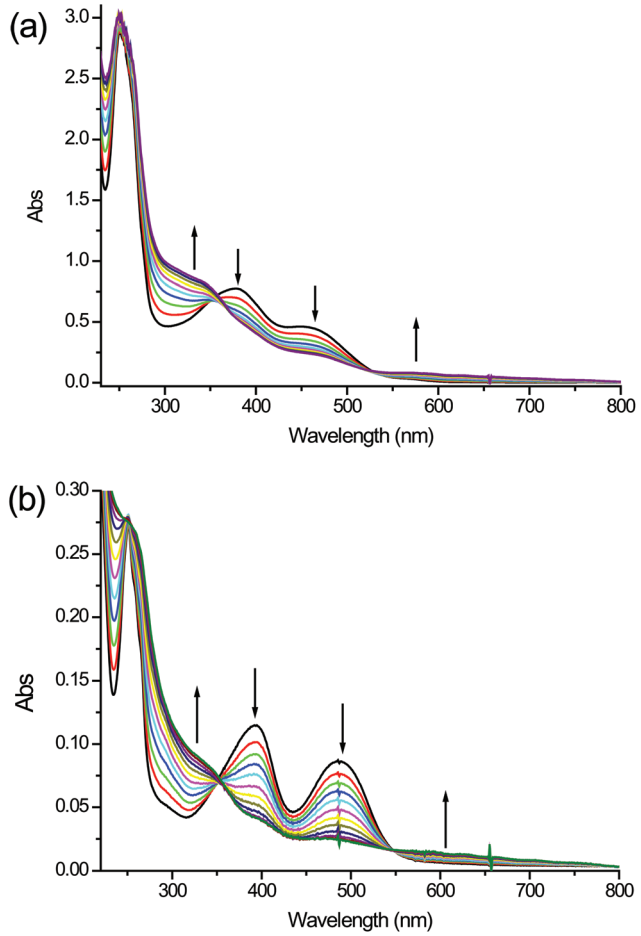

Fig. 6 Changes in UV/Vis absorption upon irradiation (at λ_{ex} = 365 nm) of (a) **1** and (b) **2** in water.

even under extended irradiation at all wavelengths, no changes were observed in the UV/Vis absorption spectra of **1** or **2**. In contrast, irradiation in all other solvents examined resulted in changes in UV/Vis absorption, EPR and resonance Raman spectra consistent with oxidation.

Photochemistry of 1 and 2 in aqueous media

Irradiation (at λ_{ex} 312 nm, 365 nm or 400 nm) of aqueous solutions of **1** and **2** resulted in a decrease in the visible absorption bands at *ca.* 390 and 450 nm, accompanied by a concomitant increase in absorption at *ca.* 320 nm and 580 nm (Fig. 6 and Fig. S10 and S11‡). Subsequent addition of L-ascorbic acid to, or electrochemical reduction of, the irradiated solution resulted in full recovery of the original UV/Vis spectra of **1** and **2** (Fig. S12‡).

The role for $^3O_2$ as electron acceptor in the photooxidation of **1** was assessed by irradiation of degassed[13] aqueous and methanol (*vide infra*) solutions of **1** at λ_{ex} 312 nm. The absorption spectra were unchanged in either solvent over 45 min of irradiation (Fig. 7). Both solutions were then purged with $^3O_2$ and irradiation continued. The bands in the visible region decreased with a concomitant increase in absorbance at *ca.* 310 nm. This demonstrates that $^3O_2$ is the terminal oxidant and that direct photolysis of solvent even under UV irradiation is not responsible for the changes observed.

Photochemistry of 1 in methanol

Irradiation (at λ_{ex} 365 nm, 400 nm or at >400 nm) of **1** in air equilibrated methanol results in oxidation as observed in water. Low intensity irradiation at λ_{ex} 312 nm (<1 mW cm^{-2}) results in a depletion of the visible absorption bands and an increase in absorption at 310 nm (Fig. 8). The X-band EPR spectrum at 77 K of the irradiated solution shows the characteristic features of a low spin Fe(III) complex with *g* values of 2.29, 2.12 and 1.95 identical to that reported for [Fe(III)(N4Py)(OMe)]$^{2+}$ (Fig. 9).[11] In addition a weak sharp signal is observed at *g* = 2.003 (*vide infra*). Addition of L-ascorbic acid to the photoproduct resulted in recovery of the initial UV/Vis absorption spectrum of **1**. Similar spectral changes were observed for samples held in the dark, albeit over 24 h (Fig. S13‡).

Irradiation of **1** in methanol at higher intensity (35 mW cm^{-2}) at λ_{ex} 400 nm (Fig. 10) results in initially similar changes to that observed at λ_{ex} 365 nm. The changes in the absorption spectrum prior to commencing irradiation (at 750 s, Fig. 10) are minor. Upon irradiation the bands 377 and 451 nm decrease in intensity, accompanied by an increase of the band at 318 nm.[14] An additional band appeared at *ca.* 590 nm, however, which is not assignable to the primary photoproduct [Fe(III)(N4Py)(OMe)]$^{2+}$ (or [Fe(III)(N4Py)(OH)]$^{2+}$, with which it is present in equilibrium). The additional spectral features are instead assigned to a secondary photoproduct formed by irradiation of the primary photoproduct. This was confirmed by irradiation of **3** (Fig. 1) in methanol at λ_{ex} 400 nm (Fig. 11 and Fig. S14‡).

Photochemistry of 2 in methanol

Irradiation of **2** in methanol resulted in similar changes in the UV/Vis absorption spectrum as observed for **1** (Fig. 12). Initially irradiation caused a small decrease in the two absorption bands in the visible region with an increase in absorption at 310 nm. Extended irradiation increased absorption in the visible region and a new band appeared at 575 nm. The time dependence of the changes in absorption shows that the band formed initially at 310 nm increases quickly, indicative for formation of the primary photoproduct. Subsequently the absorption band at 575 nm increased in intensity. Isosbestic points were not maintained in agreement with a multistep reaction. This is in contrast to **1**, for which the band at 575 nm was not observed except under irradiation at high intensity.

It is important to note that only the primary photoproduct can be formed by chemical or electrochemical oxidation and that the secondary photoproduct is not formed in the absence of light. The stability of the secondary photoproduct and its absorption spectrum confirm that it is not a peroxy[15] or higher valent (*e.g.*, Fe(IV)=O)[16] species formed by reaction with the products of the reduction of oxygen, *i.e.* superoxide or hydrogen peroxide.

The thermal and photo-stability of the secondary photoproduct of **2** in methanol is sufficient to allow for storage for several days and for resonance Raman (rR) spectra to be recorded at λ_{ex} 473 or 561 nm. rR spectra of the secondary photoproduct of **2** in

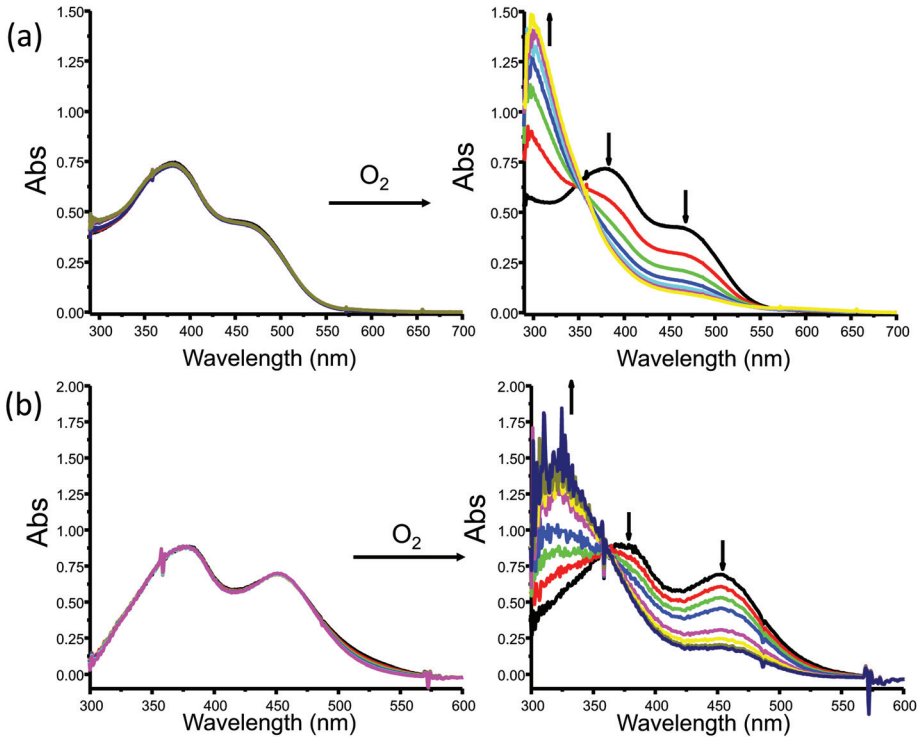

Fig. 7 Irradiation at λ_{ex} = 312 nm of **1** in (left) (a) degassed water and (b) degassed methanol for 45 min and (right) after purging with oxygen; monitored by UV/Vis absorption spectroscopy.

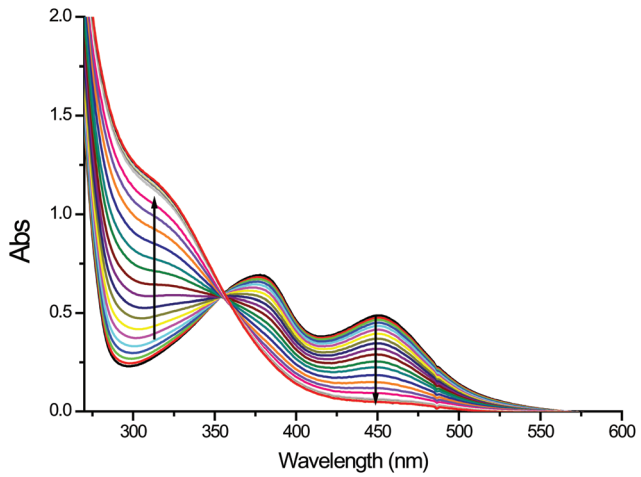

Fig. 8 Change in the UV/Vis absorption spectrum of **1** in methanol upon irradiation at λ_{ex} = 312 nm.

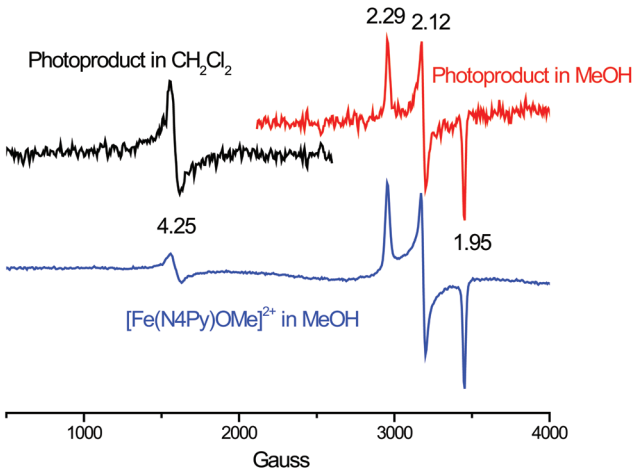

Fig. 9 EPR spectra of **3** in methanol (blue) and of the photoproduct of **1** in methanol (red, top right; from solution shown in Fig. 8) and in dichloromethane (black, top left).

methanol are shown in Fig. 13, at λ_{ex} 561 nm (*i.e.* resonant with the absorption band of the secondary photoproduct at 575 nm) and at λ_{ex} 473 nm (resonant with both **2** and the secondary photoproduct). The rR spectrum (at λ_{ex} 473 nm) of the secondary product showed differences compared to the rR spectrum of **2**, however, in general all three spectra are consistent with resonance with charge transfer transitions involving the MeN4Py ligand. Two strong bands at 681 and 651 cm^{-1} were observed in the rR spectrum of the secondary product, which are typical of Fe–O[17] or Fe–N stretching modes.[18] rR spectra of the photoproduct of **2** in d_4-methanol and ethanol show only minor differences (Fig. S15‡). Hence the absorption bands at 454 and 575 nm of the secondary photoproduct can be assigned[19] to ligand to metal charge transfer (LMCT) transitions involving at least the MeN4Py ligand.

The EPR spectra of the products of irradiation of **2** in methanol were considerably different to those obtained for **1**. The EPR spectrum after irradiation at λ_{ex} 400 nm is show in Fig. 14. A low spin Fe(III) species with *g* values (*g* = 2.29, 2.12, 1.93) consistent with the complex $[Fe(MeN4Py)(OMe)]^{2+}$ was observed. However in contrast to **1**, for **2** two additional species were

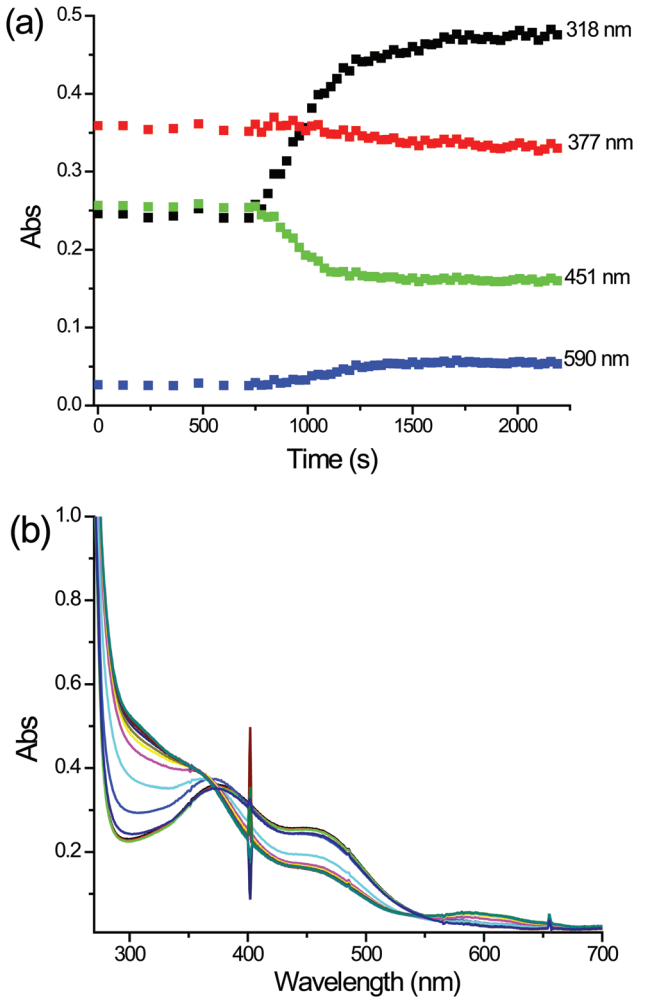

Fig. 10 Irradiation of **1** at λ_{ex} = 400 nm in methanol (a) time dependence of absorption at selected wavelengths, (b) absorption spectra over course of irradiation. Irradiation starts at 750 s. The distortion in the spectra at 400 nm is due to scattered laser light.

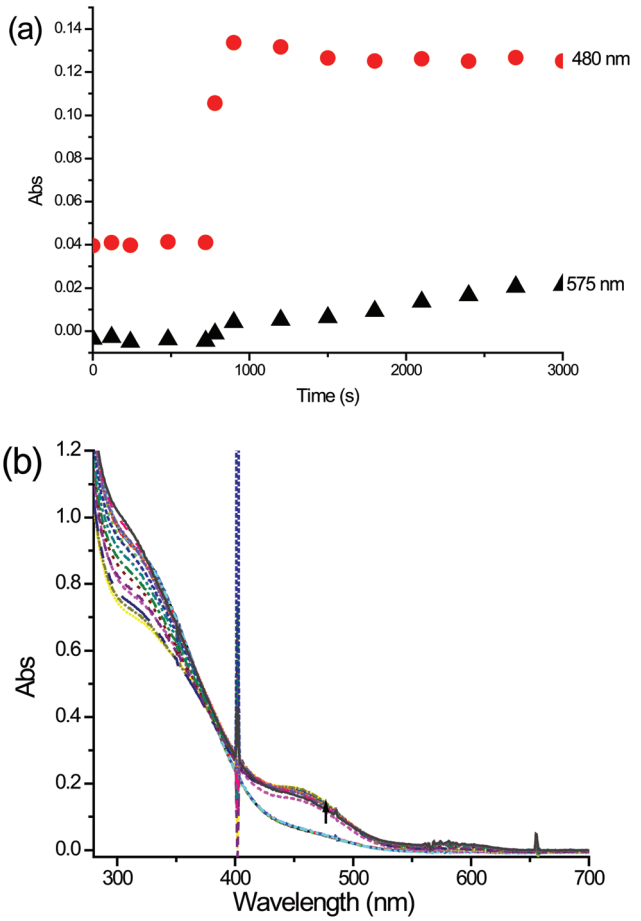

Fig. 11 Irradiation of **3** at λ_{ex} = 400 nm in methanol (a) time dependence of absorption at selected wavelengths, (b) absorption spectra over course of irradiation. Irradiation starts at 750 s. The distortion in the spectra at 400 nm is due to scattered laser light.

observed. A weak but sharp signal at g = 2.003 and a second low spin Fe(III) species with g = 1.97.

The observation of a sharp signal at g = 2.003 indicates the presence of the superoxide radical anion that forms upon electron transfer from **2** to $^3O_2$. Comparison with the EPR spectrum of KO_2 (at low concentration) in ethanol supports the assignment. The additional broad signal observed is tentatively assigned to the secondary photoproduct, which gives rise to the absorption band at 575 nm.

Photochemistry of 1 and 2 in dichloromethane

Dissolution of **1** or **2** in aqueous or methanol solution results in immediate exchange of the CH_3CN ligand for solvent. Dichloromethane is incapable of substituting the CH_3CN ligands of **1** and **2**, however residual water, if present, in dichloromethane displaces the CH_3CN ligand readily (*vide supra*).

In water-free dichloromethane, irradiation had little effect on the UV/Vis absorption spectrum consistent with the absence of photochemistry observed for **1** and **2** in acetonitrile. Addition of water to dichloromethane results in a change in the absorption spectrum of both **1** and **2**, consistent with exchange of the CH_3CN ligand with H_2O. Irradiation in the presence of water results in changes (Fig. 15 and 16, respectively) to the absorption spectrum similar to those observed in water and methanol. The absorption bands at 377 and 451 nm decreased in intensity and a strong absorption at 325 nm arises in the case of **1**. The photoproduct showed a characteristic EPR spectrum of a high spin Fe^{III} complex with a g value of 4.25 (Fig. 9). For **2**, the bands at 381 and 464 nm decreased in intensity over time and two new intense bands appeared at 325 and 355 nm.

Energy *vs.* electron transfer

Although irradiation leads to the formation of **1** and **2** in the Fe(III) redox state, this does not *a priori* mean that electron transfer from a thermally equilibrated photo-excited state is involved (*vide infra*). An alternative mechanism would be sensitised formation of $^1O_2$ followed by electron transfer. The possibility of singlet oxygen formation was investigated in dichloromethane by comparison of the intensity of singlet oxygen emission at 1260 nm (with λ_{ex} 532 nm) of isoabsorbtive solutions of **1**, **2**

and zinc-tetraphenylporphyrin (Zn-TPP). $^1O_2$ emission was observed only for the Zn-TPP and not for **1** or **2**. This indicates that the oxidation from Fe(II) to Fe(III) is a result of direct electron transfer rather than energy transfer to form singlet oxygen followed by electron transfer.

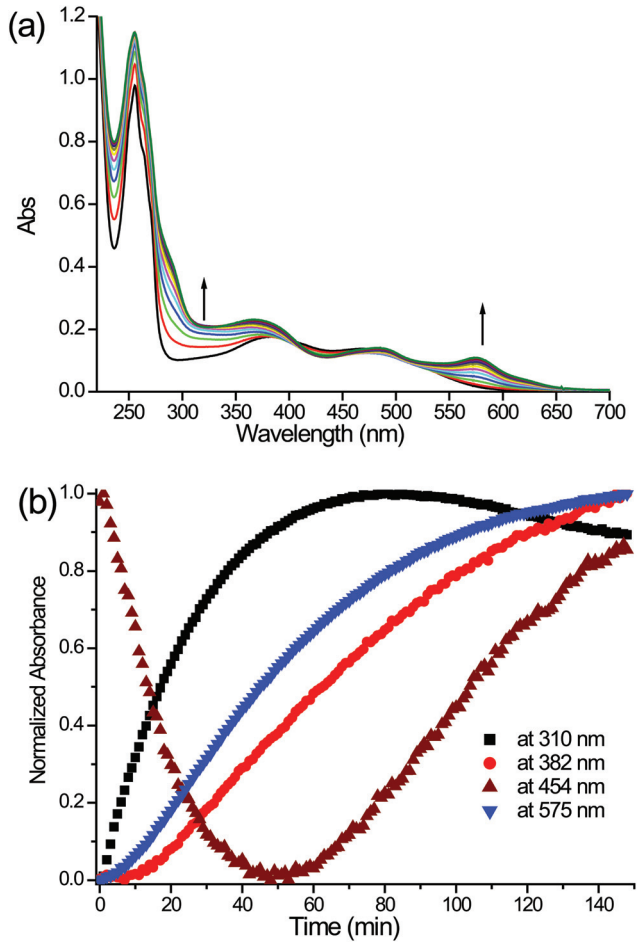

Fig. 12 (a) Changes in the UV/Vis absorption spectrum of **2** in methanol upon irradiation at λ_{ex} = 365 nm and (b) time dependence of the changes in absorbance (normalised) at selected wavelengths.

Discussion

The aim of the present study was to understand better the role of irradiation in the enhancement of the oxidative DNA cleavage activity of **1** in aqueous solution.[10] Excitation of **1** in the visible region of the electronic absorption spectrum results in population of ^{1}MLCT states that would be expected[2–5] to undergo rapid intersystem crossing (ISC) and relaxation to metal centred states before returning to the ground state. The effect of irradiation on the activity of **1** is most probably by altering its interaction with $^3O_2$. The mechanism by which **1** reacts with $^3O_2$ is not yet fully understood and can involve either (i) ligand dissociation to allow for $^3O_2$ to coordinate as proposed for iron bleomycin[20] (and hence photoinduced ligand dissociation may play a role for **1**), (ii) energy transfer to $^3O_2$ to form the highly reactive $^1O_2$ or (iii) electron transfer to $^3O_2$ to form the superoxide anion radical. Given that in aqueous or alcoholic solution ligand dissociation would be followed by rapid recomplexation by solvent and the

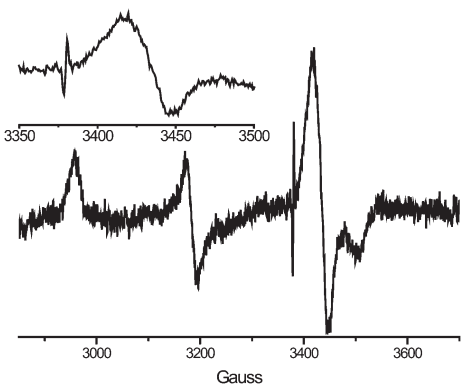

Fig. 14 EPR spectra of **2** in methanol at after irradiation at λ_{ex} = 400 nm. Inset expansion of 3350–3500 G region showing the broad signal at g = 1.97 and the sharp signal at g = 2.003.

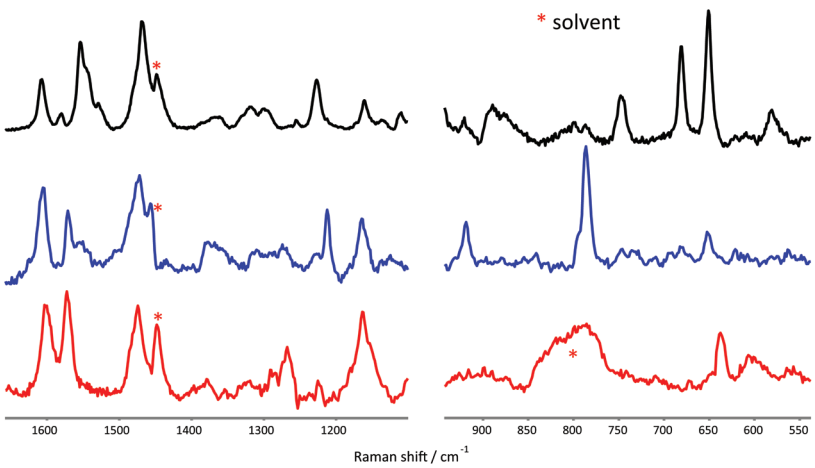

Fig. 13 Resonance Raman spectra of the secondary product of **2** in methanol at (top) λ_{ex} = 561 and (middle) λ_{ex} = 473 nm and of **2** in methanol at λ_{ex} = 473 nm. *Artefacts due to imperfect solvent subtraction.

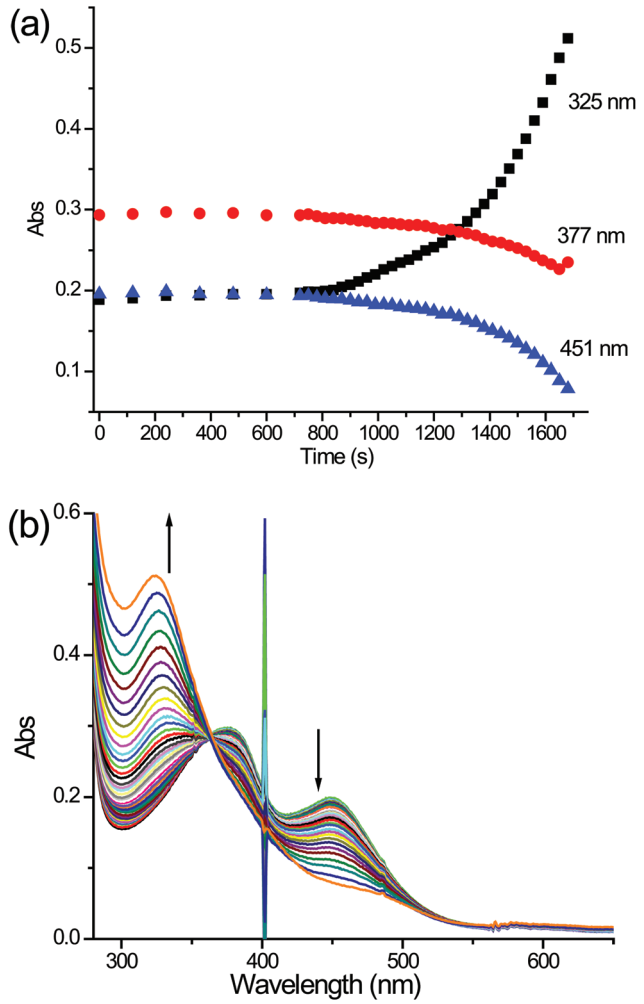

Fig. 15 Irradiation of **1** at λ_{ex} = 400 nm in dichloromethane (a) time dependence of absorption at selected wavelengths, (b) absorption spectra over course of irradiation. Irradiation starts at 750 s. The distortion in the spectra at 400 nm is due to scattered laser light.

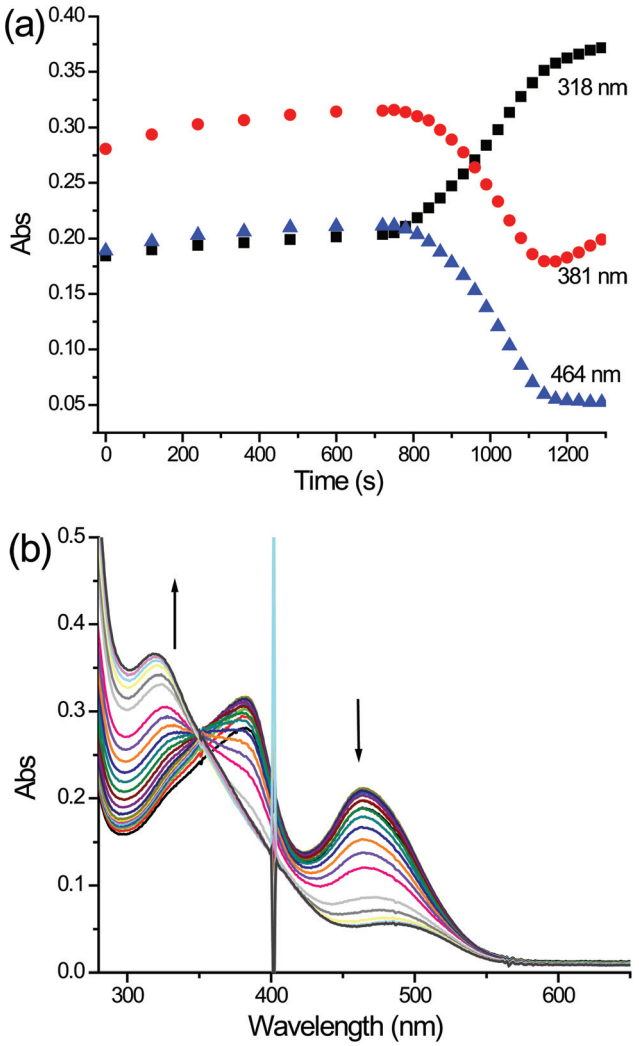

Fig. 16 Irradiation of **2** at λ_{ex} = 400 nm in dichloromethane (a) time dependence of absorption at selected wavelengths, (b) absorption spectra over course of irradiation. Irradiation starts at 750 s. The distortion in the spectra at 400 nm is due to scattered laser light.

absence of singlet oxygen emission at 1260 nm, the most likely rationalisation of the effect of irradiation is the enhancement of the rate of outer sphere electron transfer to $^3O_2$. This necessitates, however, that the involved excited state is sufficiently long lived to allow for diffusion rate limited electron transfer.

In acetonitrile (and water-free dichloromethane) complexes **1** and **2** retain the CH_3CN ligand and are diamagnetic low spin Fe(II) complexes in solution. Aerobic oxidation to the Fe(III) redox state does not occur thermally or photochemically primarily due to the high oxidation potential (*ca.* 1.1 V *vs.* Ag/AgCl) and in the latter case, possibly also due to the very short excited state lifetime. In water, methanol and water saturated dichloromethane exchange of the CH_3CN ligand for H_2O or MeOH is essentially complete. As shown previously, the aquo and hydroxido complexes of **1** and **2** exhibit two equilibria in aqueous solution: between two distinct Fe(II) species and between high and low spin states (Scheme 1). In all three solvents oxidation of **1** and **2** by $^3O_2$ proceeds under ambient conditions to yield $[Fe(III)\text{-}(R\text{-}N4Py)(OR')]^{2+}$ (where R and R′ = –H or $–CH_3$). The Fe(III) species could be generated by electrochemical or chemical oxidation also and were identified by EPR spectroscopy as a mixture of high and low spin Fe(III) species depending on pH and solvent. In general the rate of oxidation of **1** was substantially higher than the rate of oxidation of **2**, which may reflect the greater contribution of the low spin states to **2** (Scheme 1). The Fe(II) complexes could be recovered in almost all cases by electrochemical or chemical reduction.

Upon irradiation with UV or visible light in the absence of $^3O_2$, both **1** and **2** were found to be photoinert. By contrast when $^3O_2$ was present oxidation to the Fe(III) state was rapid relative to the corresponding thermal reactions. Again restoration of the Fe(II) complex could be achieved with chemical or electrochemical reduction. Importantly however the absorption bands at *ca.* 360 and 470 nm are due to the ^{1}MLCT transitions of the Fe(II) complexes in the low spin state and hence the photochemical acceleration of the oxidation of the complexes by $^3O_2$ must follow their photoexcitation. The absence of singlet oxygen emission and the anticipated short excited state lifetime of the complexes suggests that the photoinduced oxidation occurs on the ground

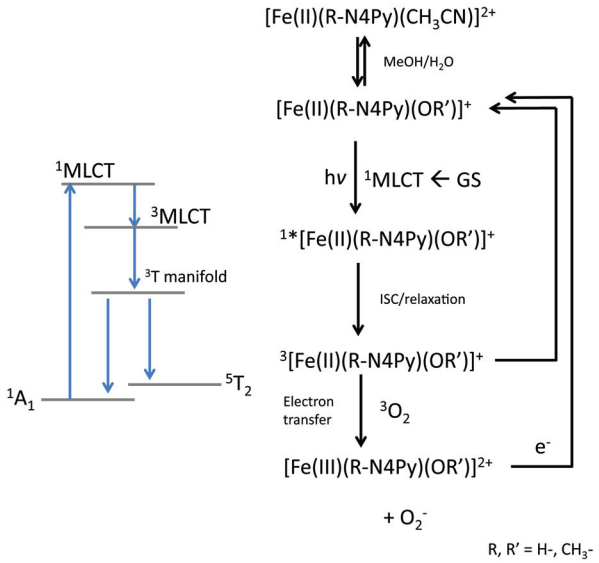

Scheme 2 Proposed mechanism for photochemically driven acceleration of the oxidation of **1** and **2** by $^3O_2$ to form the primary photoproduct.

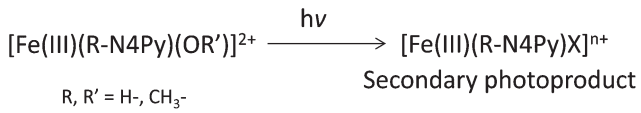

Scheme 3 The secondary photoproduct forms upon irradiation of the Fe(III) complex **3** or is formed upon irradiation of **1** and **2**, after the initial oxidation step (see Scheme 2).

state surface involving low lying spin states. That is to say that photoexcitation serves to increase the steady state population of low lying ^3T states for which the spin forbidden character for outer sphere electron transfer to $^3O_2$ is removed. Hence the effect of irradiation is at its simplest described as a perturbation of the intrinsic spin equilibria exhibited by **1** and **2** in solution. The overall mechanism is described in Scheme 2.

The first step in the mechanism is the displacement of the CH_3CN ligand with a hydroxido or methoxido ligand. The complexes formed exhibit a spin equilibrium between the $^1A_1$ and $^5T_2$ states in solution and hence transient thermal population of the $^3T_1/^3T_2$ states must occur providing a mechanism to overcome the spin forbidden character for outer sphere electron transfer to $^3O_2$. It should be noted that it is the ^{1}MLCT((Me)N4Py ← $^1A_1$) state that is populated upon photoexcitation. Hence the increased photoreactivity of **2** compared with **1** is in agreement with the increased bias towards the $^1A_1$ state for **2** in solution. Relaxation to the ground state surface is expected to be rapid in these complexes, however it is proposed here that photoexcitation serves to increase the steady state population of the intermediate ^3T states sufficiently to affect the rate of oxidation.

The observation of a sharp signal at $g = 2.003$ in the EPR spectrum of **2** in methanol after irradiation provides support to the proposed mechanism in that it is consistent with the formation of superoxide. Furthermore the proposed mechanism is consistent with the studies on the DNA cleavage activity of **1** both in the absence and presence of light.[10]

Although the focus of the present study was to examine the photochemistry of complex **1** and **2**, an interesting and somewhat surprising observation was the formation of a secondary photoproduct from the Fe(III) complex formed initially (Scheme 3). The spectroscopic properties of the secondary photoproduct are not consistent with species such as $[Fe(IV)(N4Py)(O)]^{2+}$,[16] $[Fe(III)(N4Py)(OOH)]^{2+}$ or $[Fe(III)(N4Py)(O_2)]^+$, however.[8c]

The intensity of the lowest energy absorption band, which can be assigned as an LMCT absorption involving the (Me)N4Py ligand, taken together with the recovery of **1** and **2** upon chemical reduction with L-ascorbic acid confirms that ligand oxidation, for example, is not involved and suggests that it may be a dinuclear Fe(III) complex possibly with the N4Py being tetradentate instead of pentadentate. Further studies are underway to identify these species.

Conclusions

In conclusion, the present study of the photochemically accelerated aerobic oxidation of complex **1** and **2** demonstrates the key role interconversion between the singlet and, presumably, quintet states play in the ability of **1** to interact with $^3O_2$ sufficiently to lead to oxidative DNA cleavage. The interconversion between the singlet and higher spin states would be expected to involve an intermediate triplet state, the transient formation of which would facilitate electron transfer to $^3O_2$, the first step in the cleavage of DNA by **1** with $^3O_2$. This process leads to formation of superoxide radicals that upon disproportionation form H_2O_2, which can subsequently react with **1** to form Fe–OOH species. The photoactivity of complex **3**, which is in the Fe(III) redox state to form a secondary photoproduct, raises new questions as to the photochemistry of iron complexes in general that has, perhaps, been overshadowed by their related Ru(II) complexes.

Acknowledgements

The authors thank STW (The Netherlands Foundation for Technology and Science, grant No. 11059) and NWO (The Netherlands Organisation for Science, VIDI grant No. 700.57.428, WRB) for financial support. COST action CM1003 is acknowledged for discussion also.

Notes and references

1 (*a*) P. Ceroni, G. Bergamini and V. Balzani, *Angew. Chem., Int. Ed.*, 2009, **48**, 8516; (*b*) S. Campagna, F. Puntoriero, F. Nastasi, G. Bergamini and V. Balzani, *Top. Curr. Chem.*, 2007, 117; (*c*) A. Juris, V. Balzani, F. Barigelletti, S. Campagna, P. Belser and A. von Zelewsky, *Coord. Chem. Rev.*, 1988, **84**, 85.

2 (*a*) J. K. McCusker, K. N. Walda, R. C. Dunn, J. D. Simon, D. Magde and D. N. Hendrickson, *J. Am. Chem. Soc.*, 1993, **115**, 298; (*b*) N. Huse, T. K. Kim, L. Jamula, J. K. McCusker, F. M. F. de Groot and R. W. Schoenlein, *J. Am. Chem. Soc.*, 2010, **132**, 6809; (*c*) J. K. McCusker, K. N. Walda, R. C. Dunn, J. D. Simon, D. Magde and D. N. Hendrickson, *J. Am. Chem. Soc.*, 1993, **115**, 298.

3 (*a*) A. Cannizzo, C. J. Milne, C. Consani, W. Gawelda, C. Bressler, F. van Mourik and M. Chergui, *Coord. Chem. Rev.*, 2010, **254**, 2677; (*b*) C. Bressler, C. Milne, V.-T. Pham, A. Elnahhas, R. M. van der Veen, W. Gawelda, S. Johnson, P. Beaud, D. Grolimund, M. Kaiser, C. N. Borca, G. Ingold, R. Abela and M. Chergui, *Science*, 2009, **323**, 489; (*c*) W. Gawelda, A. Cannizzo, V. T. Pham, F. van Mourik, C. Bressler and M. Chergui, *J. Am. Chem. Soc.*, 2007, **129**, 8199.

4 (*a*) J. A. Wolny, H. Paulsen, J. J. McGarvey, R. Diller, V. Schunemann and H. Toftlund, *Phys. Chem. Chem. Phys.*, 2009, **11**, 7562; (*b*) C. Brady, P. L. Callaghan, Z. Ciunik, C. G. Coates, A. Dossing, A. Hazell, J. J. McGarvey, S. Schenker, H. Toftlund, A. X. Trautwein, H. Winkler and J. A. Wolny, *Inorg. Chem.*, 2004, **43**, 4289; (*c*) S. Schenker, P. C. Stein, J. A. Wolny, C. Brady, J. J. McGarvey, H. Toftlund and A. Hauser, *Inorg. Chem.*, 2001, **40**, 134; (*d*) A. H. R. Alobaidi, J. J. McGarvey, K. P. Taylor, S. E. J. Bell, K. B. Jensen and H. Toftlund, *J. Chem. Soc., Chem. Commun.*, 1993, 536.

5 (*a*) C. Creutz, M. Chou, T. L. Netzel, M. Okumura and N. Sutin, *J. Am. Chem. Soc.*, 1980, **102**, 1309; (*b*) C. Brady, J. J. McGarvey, J. K. McCusker, H. Toftlund and D. N. Hendrickson, *Top. Curr. Chem.*, 2004, **235**, 1.

6 (*a*) A. Hauser, C. Enachescu, M. L. Daku, A. Vargas and N. Amstutz, *Coord. Chem. Rev.*, 2006, **250**, 1642; (*b*) A. Hauser, *Top. Curr. Chem.*, 2004, **234**, 155; (*c*) R. Hinek, H. Spiering, P. Gutlich and A. Hauser, *Chem.–Eur. J.*, 1996, **2**, 1435.

7 (*a*) J. Torres-Alacan, O. Krahe, A. C. Filippou, F. Neese, D. Schwarzer and P. Vçhringer, *Chem.–Eur. J.*, 2012, **18**, 3043; (*b*) C. R. Child, S. Kealey, H. Jones, P. W. Miller, A. J. P. White, A. D. Gee and N. J. Long, *Dalton Trans.*, 2011, **40**, 6210; (*c*) N. G. Tran, H. Kalyvas, K. M. Skodje, T. Hayashi, P. Moenne-Loccoz, P. E. Callan, J. Shearer, L. J. Kirschenbaum and E. Kim, *J. Am. Chem. Soc.*, 2011, **133**, 1184.

8 (*a*) M. Lubben, A. Meetsma, E. C. Wilkinson, B. L. Feringa and L. Que Jr., *Angew. Chem., Int. Ed. Engl.*, 1995, **34**, 1512; (*b*) G. Roelfes, M. E. Branum, L. Wang, L. Que Jr. and B. L. Feringa, *J. Am. Chem. Soc.*, 2000, **122**, 11517; (*c*) G. Roelfes, V. Vrajmasu, K. Chen, R. Y. N. Ho, J. Rohde, C. Zondervan, R. M. la Crois, E. P. Schudde, M. Lutz, A. L. Spek, R. Hage, B. L. Feringa, E. Münck and L. Que Jr., *Inorg. Chem.*, 2003, **42**, 2639.

9 A. Draksharapu, Q. Li, H. Logtenberg, T. A. van den Berg, A. Meetsma, J. S. Killeen, B. L. Feringa, R. Hage, G. Roelfes and W. R. Browne, *Inorg. Chem.*, 2012, **51**, 900.

10 (*a*) Q. Li, W. R. Browne and G. Roelfes, *Inorg. Chem.*, 2010, **49**, 11009; (*b*) Q. Li, W. R. Browne and G. Roelfes, *Inorg. Chem.*, 2011, **50**, 8318.

11 G. Roelfes, M. Lubben, K. Chen, R. Y. N. Ho, A. Meetsma, S. Genseberger, R. M. Hermant, R. Hage, S. K. Mandal, V. G. Young, Y. Zang, H. Kooijman, A. L. Spek, L. Que and B. L. Feringa, *Inorg. Chem.*, 1999, **38**, 1929.

12 M. Krejčík, M. Daněk and F. Hartl, *J. Electroanal. Chem. Interfacial Electrochem.*, 1991, **317**, 179.

13 Solutions were degassed by four freeze–pump–thaw cycles.

14 The photochemical quantum yield for the photooxidation of **1** can be roughly estimated at *ca*. 0.01 from these data, however the exact value is expected to be highly dependent on concentration of both the complex and oxygen as well as temperature.

15 M. Lubben, A. Meetsma, E. C. Wilkinson, B. L. Feringa and L. Que Jr., *Angew. Chem., Int. Ed. Engl.*, 1995, **34**, 1512.

16 J. Kaizer, E. J. Klinker, N. Y. Oh, J.-U. Rohde, W. J. Song, A. Stubna, J. Kim, E. Muenck, W. Nam and L. Que Jr., *J. Am. Chem. Soc.*, 2004, **126**, 472.

17 J.-J. Girerd, F. Banse and A. J. Simaan, *Struct. Bonding*, 2000, **97**, 145.

18 (*a*) R. Y. N. Ho, G. Roelfes, B. L. Feringa and L. Que Jr., *J. Am. Chem. Soc.*, 1999, **121**, 264; (*b*) R. Y. N. Ho, G. Roelfes, R. M. Hermant, R. Hage, B. L. Feringa and L. Que Jr., *Chem. Commun.*, 1999, 2161.

19 M. R. Bukowski, S. R. Zhu, K. D. Koehntop, W. W. Brennesse and L. Que Jr., *J. Biol. Inorg. Chem.*, 2004, **9**, 39.

20 (*a*) R. M. Burger, S. B. Horwitz, J. Peisach and J. B. Wittenberg, *J. Biol. Chem.*, 1983, **258**, 1559; (*b*) R. M. Burger, T. A. Kent, S. B. Horwitz, E. Munck and J. Peisach, *J. Biol. Chem.*, 1983, **258**, 1559.

